Applied Radiation and Isotopes 121 (2017) 122–125

Contents lists available at ScienceDirect

Applied Radiation and Isotopes

journal homepage: www.elsevier.com/locate/apradiso

# Effects of micro-sized and nano-sized $WO_3$ on mass attenauation coefficients of concrete by using MCNPX code

H.O. Tekin[a,*], V.P. Singh[b], T. Manici[c]

[a] Uskudar University, Vocational School of Health Services, Radiotherapy Department, İstanbul 34672, Turkey
[b] Department of Physics, Karnatak University, Dharwad, 580 003, India
[c] Uskudar University, Medical Radiation Research Center (USMERA), Istanbul 34672, Turkey

ARTICLE INFO

*Keywords:*
Nanoparticles
Concrete
Shielding
Radiation protection
MCNPX

ABSTRACT

In the present work the effect of tungsten oxide ($WO_3$) nanoparticles on mass attenauation coefficients of concrete has been investigated by using MCNPX (version 2.4.0). The validation of generated MCNPX simulation geometry has been provided by comparing the results with standard XCOM data for mass attenuation coefficients of concrete. A very good agreement between XCOM and MCNPX have been obtained. The validated geometry has been used for definition of nano-$WO_3$ and micro-$WO_3$ into concrete sample. The mass attenuation coefficients of pure concrete and $WO_3$ added concrete with micro-sized and nano-sized have been compared. It was observed that shielding properties of concrete doped with $WO_3$ increased. The results of mass attenauation coefficients also showed that the concrete doped with nano-$WO_3$ significanlty improve shielding properties than micro-$WO_3$. It can be concluded that addition of nano-sized particles can be considered as another mechanism to reduce radiation dose.

## 1. Introduction

The radiation protection is a cutting edge field of investigation for radiation measurement, shielding, interaction of radiation with human organs and appropriate utilisation of information to protect the people and staff from ionizing radiation. The investigations on radiation shielding materials and equipments acquired much interest due to technological developments and extensive using fields of ionizing radiation in nuclear technology, medical, agriculture, industries, etc. Radiation exposure occurs for staff and patients in different environments such as medical radiation facilities, nuclear reactors, accelerators and radioisotopic facilities. Therefore, potential radiation exposure are minimized by applying as low as reasonably achievable (ALARA) principle and three main rules such as time, distance and shielding. Time and distance are managable parameters by individual to control radiaiton exposure. However, third of the main rules namely shielding which should be pre-decided for radiation facilities. The shielding of facility, equipments and components requires some kinds of investigation results to decide for implementation. Therefore, the radiation shielding requires investigation on various types materials, compounds, mixtures to provide maximum protection from radiaiton. Various theoretical, experimental and simulation investigations on shieldng materials are found in literature. The attenuation features of radiation for a specific target environment are required to determine the amount of shielding necessary (Kanwaldeeo et al., 2015). The mass attenuation coefficient ($\mu_m$) is one of the fundamental interaction parameters for a material (shielding, dosimetric). The $\mu_m$ for characterizes the penetration and diffusion of gamma ray in attenuator material (Abdel-Rahman et al., 2000). The $\mu_m$ is a density independent coefficient and determined for attenuator material by using the transmission method by Lambert-Beer law which is formulated as $\mu_m x = \ln (I_0/I)$. Where $I_0$ and I are the incident and attenuated photon intensity, respectively. The $\mu_m$ ($cm^2\,g^{-1}$) is the mass attenuation coefficient and x is the thickness of the attenuator slab. The shielding method is mostly depending on radiation energy and charge of shielding materials. On the other hand, choice of shielding material depends on material features such as type of radiation, system requirement, strength to radiation damage, economic conditions and mechanical properties (Hassan et al., 2015).

Concrete and lead based products have been widely used in different kind of radiation facilities due to its specific properties for protection against radiation. Concrete is selected for shielding of photon and neutron because of it is mixture of low- and high-atomic number elements. Lead is found one of the suitable option for shielding against X- and gamma-rays, though it is found carcinogenic material. Due to enormous applications of nano-materials, nowadays, use of the

* Corresponding author.
*E-mail address:* huseyinozan.tekin@uskudar.edu.tr (H.O. Tekin).

http://dx.doi.org/10.1016/j.apradiso.2016.12.040
Received 26 August 2016; Received in revised form 31 October 2016; Accepted 18 December 2016
Available online 21 December 2016

nano-sized particles in materials has fascination for researches due to various features (Noor Azman et al., 2013). The main goal of investigations on nano-sized particles is to understand the behaviour of matter at the nanoscales from 1 nm to 100 nm. The features of nano-sized particles are novel and can be engineered by managing the dimensions (Singh et al., 2011). Tungsten oxide ($WO_3$) is a transition metal oxide semiconductor in the range of Eg = 2.5–2.8 eV at room temperature with 7.16 g/cm$^3$ density (d). Various studies in different fields have been reported regarding the usage of nano-$WO_3$ in literature. Carbon nanotube have been investigated for transmission of X-ray and higher mass attenuation coefficients was observed. Synthesis of tungsten oxide nanoparticles by acid precipitation method has been studied by Sitthisuntorn et al. (2007)). Optical properties of colloidal $WO_3$ nanorods have been studied by Lee et al. (2003). The usage conditions of nano-$WO_3$ as a catalyst for malonic acid ester synthesis have been studied by Wasmi et al. (2014). The potential applications as thermal insulation coatings for building and car glasses have been studied Jing-xiao et al. (2014). Preparation and application of nano $WO_3$ to $NO_2$ sensor has been studied by Meng et al. (2009). Electrodeposition of $WO_3$ nanoparticles for sensing applications has been studied by Santos et al. (2015). On the other hand, it is extensively believed that in nano-dimensional sizes, particles are more regular and have less agglomerations in material and thus it can improve the attenuation ability of material (Botelho et al., 2011; El Haber and Froyer, 2008). Noor Azman et.al investigated the radiation attenuation properties of nano-$WO_3$ added epoxy and reported that effect of particle size was more pronounced at lower radiation energies (Noor Azman and Siddiqui, Low). New type of nano-sized particle added shielding materials have been reported by different researchers. However, simulation on nano-sized particle added shielding materials are not found in literature. This has encourages us to investigate in detail for micro-sized and nano-sized particle added shielding materials using simulation tool. Since concrete is the one of most used building material in radiation and nuclear facilities (PET, CT scan, X-ray, nuclear medicine, nuclear reactors, accelerators, isotope handling), therefore concrete was selected for investigation on doping with micro- $WO_3$ and nano-$WO_3$.

Hence, this study aimed to investigate the effect of nano-$WO_3$ in concrete sample and compare the results with micro-$WO_3$ added concrete sample by using Monte Carlo method. In addition, this study aimed not only to verify the increasing effect of nano-$WO_3$ on radiation attenuation process and compare the increase rates on radiation attenuation with previous experimental studies which experimentally studied for different attenuator materials such as epoxy (Dong et al., 2012) but also investigate the abilities of MCNPX code during the investigations of nano-sized particles. This study would be very useful for wide applications of nano-sized particle added shielding materials and utilisation of standardised geometry of Monte Carlo simulation for medical physics, radiation physics, shielding and radiation protection.

## 2. Materials and methods

### 2.1. MCNPX simulation geometry

MCNPX is a radiation transport code for modeling the interaction of radiation with materials and also tracks all particles at different energies. MCNPX is fully three-dimensional and it utilizes extended nuclear cross section libraries and uses physics models for particle types (RSICC Computer Code Collection, 2002). Different studies about abilities of MCNPX have been reported. Availability of MCNPX on detection efficiency and using of different experimental and Monte Carlo studies has been studied by Akkurt et al. (2015). Also using conditions of MCNPX for dose distribution has been studied by Tekin et.al (Tekin and Kara, 2016). The total simulation geometry is seen in Fig. 1 and as it can be seen, one cylindrical 3 × 3 in. NaI (Tl) detector of height in crystal 7.62 cm and diameter 7.62 cm and with a mono-

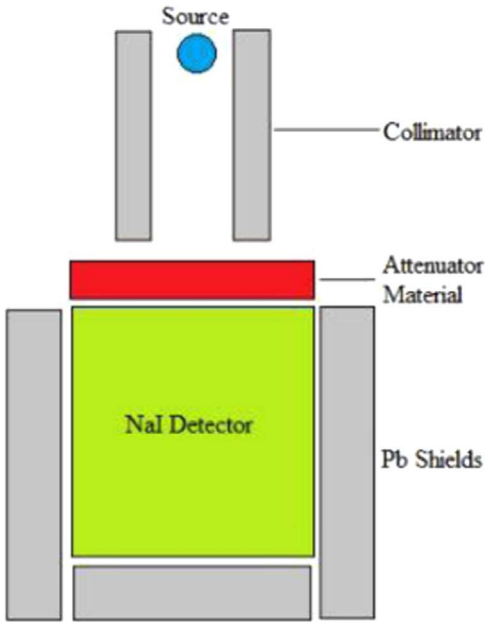


**Fig. 1.** Simulation geometry of valiation calculations.

energetic isotropic point source (Tekin, 2016). In this study, each surfaces have been defined in input file by considering the geometric dimensions and coordinates and each cells have been defined by considering the density and material contents. The expected particle counting in the simulation has been selected as photon (par = 2). This type of approach is a one of important variance reduction to reduce statistical error and optimise the computer processor by ignoring the unused particle counting for output data.

### 2.2. Definiton of micro and nanoparticles in MCNPX code

The nano-$WO_3$ have been defined into concrete sample in MCNPX input file. In this study, each nano particle voids have been defined by using the lattice (LAT) and universe (u) properties of MCNPX. The definition of each nanoparticle into the concrete sample has been considered for 100 nm diameter of $WO_3$ sphere geometry into an edge of 2 μm cube and the definition of each microparticle into the concrete sample has been considered for 1 μm diameter of $WO_3$ sphere geometry into an edge of 2 μm cube, respectively. The lead attenuator material has been modeled as 8 × 8 × 2 cm cube so $1{,}6 \times 10^{13}$ nano-$WO_3$ and micro-$WO_3$ have been added inside of lead. Doping of the $WO_3$ particles into the concrete sample has caused an increase in density. The schematic view of nano-$WO_3$ added target can be seen in Fig. 2 with defined sphere nano geometries into cubes. Gamma-ray source, lead (density = 11,34 g/cm$^3$) collimators, concrete sample target material (density = 2,26 g/cm$^3$) and 3 × 3 in. NaI (Tl) detector have been defined in cell card, surface card and data card sections of MCNPX input by considering different variable such as CEL, ERG, DIR, POS, and PAR.

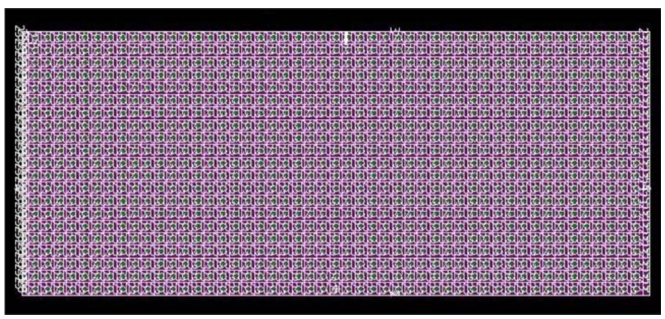

**Fig. 2.** Schematic view of nano-WO3 in attenuator material (MCNPX screenshot).

The geometric center of detector cell has been considered for location of point source. On the other hand, one of important definition is material definition by considering atomic number, mass number and density (d) for pure materials and atomic number, elemental mass concentrations and density for compounds or mixtures. By considering these parameters, we defined firstly the pure concrete sample and secondly $WO_3$ nanoparticles added concrete sample in input file respectively. In the MCNPX simulation process $10^6$ photons were used as a number of particle. To acquire absorbed dose amount in $3\times3$ in. NaI (Tl), energy deposition mesh tally (F6) has been used. This type of tally in MCNPX scores energy deposition data in which energy deposited per unit volume from all particles is included. MCNPX calculations were completed by using Intel® Core ™ i7 CPU 2.80 GHz computer hardware.

## 3. Results and discussion

### 3.1. Validation of simulation geometry

In this study, a simulation geometry has been generated by using the same physical parameters of experimental tools to verify the validation of our simulation input file. For this aim, the mass attenuation coefficients of concrete sample have been calculated and compared with XCOM data (Berger and Hubbell, 1987). The mass attenuation coefficients of concrete sample were measured for gamma rays of different energies which have been obtained from widely used $^{137}$Cs, $^{60}$Co and $^{152}$Eu point sources. The elemental mass fractionss of simple concrete (Sharaf and Hamideen, 2013) were presented in Table 1. Table 2 shows the calculated mass attenuation coefficients of concrete sample and photon energies by giving calculated values by the XCOM database and the deviations ($D=E_a–E_b/E_b\times100\%$) between this study and XCOM data. During the validation study the error rate has been observed less than %1 in output file. As it can be seen from Fig. 3, we achieved a significantly good agreement between MCNPX and XCOM data. The standard deviation rates obtained in the range of 0,3365 to 1,2179. Therefore, the modeled MCNPX simulation geometry input has been confirmed as a validated input and then considered as a standard and usable simulation input for the definition of nanoparticles in MCNPX Fig. 4.

### 3.2. Effect of nano-$WO_3$ on mass attenuation properties of concrete

The size effect of $WO_3$ particles on the mass attenuation coefficients of concrete sample has been investigated. The validated and standard input file has been used to definiton of micro-$WO_3$ and nano- $WO_3$ into the concrete sample. The definition of micro-$WO_3$ has been considered as mass fractional mixture in the range of % 50 $WO_3$ and % 50 concrete. The definition of mixture has been performed as usual mixture definition in MCNPX. The mass attenuation coefficients of micro-$WO_3$ and concrete mixture have been calculated at photon energies of 663 keV, 778,6 keV, 964 keV, 1112 keV, 1170 keV, 1330 keV, 1407 keV. The results for mass attenuation coefiicients of micro-$WO_3$ and concrete mixture have been observed higher than pure concrete. In the MCNPX simulation process $10^6$ photons were used as a number of particle. After the calculations of mass attenuation coefiicients of micro-$WO_3$, the same calculation parameters have been used for the results for mass attenuation coefiicients of nano-$WO_3$ and concrete mixture. The calculated results for mass attenuation coefficients of pure concrete, micro-$WO_3$ concrete mixture and nano-$WO_3$ concrete mixture presented in Table 3. As shown in Table 3, there was an obvious difference in mass attenuation coefficients of pure concrete, micro-$WO_3$ concrete mixture and nano-$WO_3$ concrete mixture. According to the results presented in Table 3, it is possible to express that mass attenuation

**Table 1**
Elemental mass fractionss of concrete (d = 2,26 g/cm$^3$).

| Element | Concentration |
|---|---|
| H | 0 |
| C | 0 |
| O | 0.492 |
| Na | 0.005 |
| Mg | 0.003 |
| Al | 0.037 |
| Si | 0.37 |
| P | 0 |
| S | 0 |
| K | 0 |
| Ca | 0.082 |
| Ti | 0 |
| Mn | 0 |
| Fe | 0.011 |

**Table 2**
Mass attenuation coefficients for the concrete sample ($\mu_m$ cm$^2$ g$^{-1}$).

| Energy (keV) | This Study (MCNPX) | XCOM | Deviation ($D=E_a-E_b/E_b\times100\%$) |
|---|---|---|---|
| 663 | 0,07812 | 0,07718 | 1,2179 |
| 778,6 | 0,07198 | 0,07163 | 0,4886 |
| 964 | 0,06521 | 0,0647 | 0,7882 |
| 1112 | 0,06083 | 0,06029 | 0,8956 |
| 1170 | 0,05922 | 0,05868 | 0,9202 |
| 1330 | 0,05534 | 0,05499 | 0,6364 |
| 1407 | 0,05366 | 0,05348 | 0,3365 |

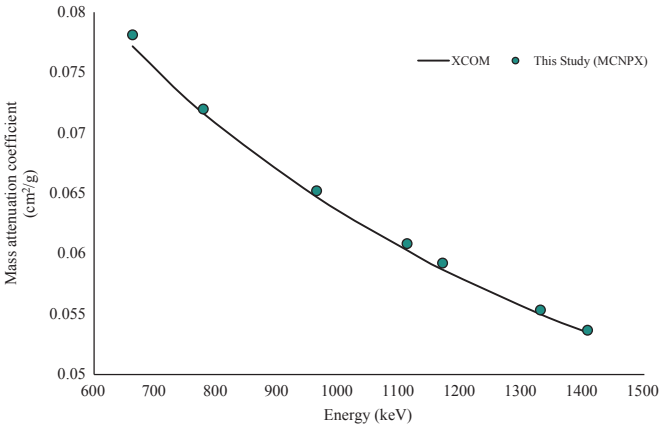


**Fig. 3.** MCNPX and XCOM data comparison for mass attenuation coefficients of concrete.

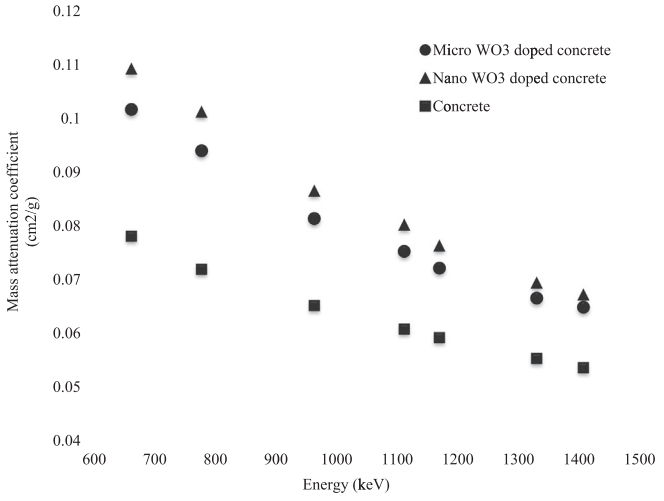


**Fig. 4.** Comparison of mass attenuation coefficients of concrete among pure concrete, micro-$WO_3$, nano-$WO_3$ concrete.

**Table 3**
Mass attenuation coefficients for the concrete, micro-$WO_3$ and nano-$WO_3$ ($\mu_m$ $cm^2$ $g^{-1}$).

| Energy (keV) | Concrete | Micro-$WO_3$ doped concrete | Nano-$WO_3$ doped concrete |
|---|---|---|---|
| 663 | 0,07812 | 0,1017 | 0,1092 |
| 778,6 | 0,07198 | 0094 | 0,1012 |
| 964 | 0,06521 | 0,0814 | 0,0865 |
| 1112 | 0,06083 | 0,0753 | 0,0802 |
| 1170 | 0,05922 | 0,0722 | 0,0763 |
| 1330 | 0,05534 | 0,0666 | 0,0694 |
| 1407 | 0,05366 | 0,0649 | 0,0672 |

**Table 4**
The percentage of the mass attenuation increase rates for different energies.

| Energy (keV) | Micro-$WO_3$ | Nano-$WO_3$ | Attenuation Increase from Micro-$WO_3$ to Nano-$WO_3$ (%) |
|---|---|---|---|
| 663 | 0,1017 | 0,1098 | 7,96 |
| 778,6 | 0094 | 0,1012 | 7,65 |
| 964 | 0,0814 | 0,0869 | 6,75 |
| 1112 | 0,0753 | 0,0802 | 6,50 |
| 1170 | 0,0722 | 0,0763 | 5,67 |
| 1330 | 0,0666 | 0,0694 | 4,20 |
| 1407 | 0,0649 | 0,0672 | 3,54 |

coefficients of concrete have increased with micro-$WO_3$ and nano-$WO_3$ doping. Somehow, mentioned increase have not been observed in same range at different energies. Due to different photon interactions occurs in different gamma energies such as photoelectric effect and compton scattering, the attenuation enhancement decreases for higher energies. It is obvious from the Table 3 that nano-$WO_3$ concrete mixture has a higher mass attenuation coefficients and increased the shieldng capability of concrete. In addition, from this investigation it can be concluded that smaller size of $WO_3$ can give the better shielding property to the concrete sample. The increasing attenuation rates between micro-$WO_3$ and nano-$WO_3$ have been calculated by using the formula (1) below. Thus, the percent of the increased attenuation rates at 663 keV, 778,6 keV, 964 keV, 1112 keV, 1170 keV, 1330 keV, 1407 keV photon energies tabulated in Table 4. According to Table 4, the maximum attenuation increase has been observed at 1407 keV photon energy. It is obvious that attenuation increase rates have changed from %3,54 to %7,96.

$$\delta = \frac{\mu nano - \mu micro}{\mu micro} x100\% \quad (1)$$

However, various studies on effect of $WO_3$ particle size for better radiation attenuation have been reported in literature. Dong et.al (2012) have reported that from the shielding point of view the nano-$WO_3$ is more effective than micro-$WO_3$ in the epoxy resin based radiation shielding material. Noor Azman et.al (2013) have reported that size effect was more pronounced at lower synchrotron radiation energies (10–20 keV) since the X-ray transmission in nano-sized $WO_3$-epoxy composites was less than in their microsized counterparts. Kim et al. (2014) reported that attenuation of gammas for the nano-W composites was enhanced up to ~75% for Ba-133 (~0.3 MeV) compared to the micro-W for polymer composites, while it decreases as the photon energy increases and MCNP simulation also shows similar gamma attenuation behaviors. However, they reached that MCNP simulation results have agreed well with experimental results by showing similar gamma attenuation behaviors. Tekin et al. (2016) reported that nano-$BaSO_4$ doped lead increased the amount of absorbed radiation in the attenuator material. In this study, similar effects of nano-$WO_3$ also have been observed precisely for the concrete material.

## 4. Conclusion

In this study, the mass attenuation coefficients of concrete by nano-$WO_3$ and micro-$WO_3$ have been investigated. It was found that size of the $WO_3$ affected the mass attenuation coefficients of concrete in all photon energies. The results indicated that nano-sized particles have greater attenuation properties compared the micro-sized particles. Due to the smaller sizes of the nano particles, the crackle is blocked more efficiently. The concrete doped with nano-$WO_3$ significanlty improve shielding properties than micro-$WO_3$. On the other hand, MCNPX is a strong and effective tool for investigations on nano-sized materials where experimental results are not available. It can be also concluded that investigated standart MCNPX geometry can be used for potential future studies since nano technology is also recently used for production of various radiation shields and technologies.

## References


Abdel-Rahman, M.A., Badawi, E.A., Abdel-Hady, Y.L., Kamel, N., 2000. Effect of sample thickness on the measured mass attenuation coefficients of some compounds and elements for 59.54, 661.6 and 1332.5 keV c-rays. Nucl. Instrum. Methods Phys. Res. A 447, 432–436.

Akkurt, I., Tekin, H.O., Mesbahi, A., 2015. Calculation of Detection Efficiency for the Gamma Detector using MCNP-X. Acta Phys. Pol. A 128 (2-B), 332–334, (DOI:10.12693(APhysPolA.128.B-332).

Berger, M.J., Hubbell, J.H., 1987. XCOM: photon cross sections database, web version 1.2, 1999. Originally Published as NBSIR 87-3597 XCOM: Photon Cross Sections on a Personal Computer, Washington, DC. Available from: ⟨http://physics.nist.gov/xcom⟩.

Botelho, M.Z., Kunzel, R., Okuno, E., Levenhagen, R.S., Basegio, T., Bergmann, C.P., 2011. X-ray transmission through nanostructured and microstructured CuO materials. Appl. Radiat. Isot. 69, 527–530.

Dong, Y., Chang, S.-Q., Zhang, H.-X., Ren, C., Kang, B., Dai, M.-Z., Dai, Y.-D., 2012. Effects of WO3 particle size in WO3/epoxy resin radiation shielding material. Chin. Phys. Lett. 29 (10), 108102.

El Haber, F., Froyer, G., 2008. Transparent polymers embedding nanoparticles for X-rays attenuation. J. Univ. Chem. Technol. Metall. 43, 283–290.

Hassan, H.E., Badran, H.M., Aydarous, A., Sharshar, T., 2015. Studying the effect of nano lead compounds additives on the concrete shielding properties for γ-rays. Nucl. Instrum. Methods Phys. Res. B 360, 81–89.

Jing-xiao, L., Qiang, X., Fei, S., Suhua, L., Jiayu, L., Lei, B., Xiang, F., 2014. Dispersion of Cs0.33WO3particles for preparing its coatings with higher near infrared shielding properties. Appl. Surf. Sci. 309, 175–180.

Kanwaldeeo, S., Sukhpal, S., Dhaliwal, A.S., Gurmel, S., 2015. Gamma radiation shielding analysis of lead-flyash concretes. Appl. Radiat. Isot. 95 (2015), 174–179.

Kim, J., Lee, B.-C., Miller, W.H., 2014. Nano-W dispersed gamma radiation shielding materials. Adv. Eng. Mater. 16 (9), 1083–1089.

Lee, K., Seo, W.S., Park, J.T., 2003. Synthesis and optical properties of colloidal tungsten oxide nanorods. J. Am. Chem. Soc. 125 (12), 3408–3409. http://dx.doi.org/10.1021/ja034011e.

Meng, D., Yamazaki, T., Yanbai, S., Zhifu, L., Toshio, K., 2009. Preparation of WO3 nanoparticles and application to NO2 sensor. Appl. Surf. Sci. 256, 1050–1053.

Noor AzmanN.Z., SiddiquiS.A., LowI.M., Characterisation of micro-sized and nano-sized tungsten oxide-epoxy composites for radiation shielding of diagnostic X-rays. Mater. Sci. Eng. C. vol. 33(8), pp. 4952–4957.

Noor Azman, N.Z., Siddiqui, S.A., Hart, R., Low, I.M., 2013. Effect of particle size,filler loadings and x-ray tube voltage on the transmitted x-ray transmission in tungsten oxide-epoxy composites. Appl. Radiat. Isot. 71, 62–67.

RSICC Computer Code Collection, 2002. MCNPX User's Manual Version 2.4.0. Monte Carlo N-Particle Transport Code System for Multiple and High Energy Applications.

SantosL., NetoJ.P., CrespoA., BaiãoP., BarquinhaP., PereiraL., MartinsR., FortunatoE., 2015. Electrodeposition of WO3 Nanoparticles for Sensing Applications. Nanotechnology and Nanomaterials Electroplating of Nanostructures. Chapter 2. Publisher: InTech. ISBN 978-953-51-2213-5.

Sharaf, J.M., Hamideen, M.S., 2013. Photon attenuation coefficients and shielding effects of Jordanian building materials. Ann. Nucl. Energy 62, 50–56.

Singh, Manoj, Manikandan, S., Kumaraguru, A.K., 2011. Nanoparticles: a new technology with wide applications. Res. J. Nanosci. Nanotechnol 1, 1–11.

Sitthisuntorn, S., Panpailin, S., Sorachon, Y., Mana, S., 2007. Synthesis of tungsten oxide nanoparticles by acid precipitation method. Ceram. Int. 33, 931–936.

TekinH.O., MCNP-X Monte Carlo Code Application for Mass Attenuation Coefficients of Concrete at Different Energies by Modeling 3×3 in. NaI(Tl) Detector and Comparison with XCOM and Monte CarloData. Science and Technology of Nuclear Installations. Volume 2016Article ID 6547318, 7 pages. ⟨http://dx.doi.org/10.1155/2016/6547318⟩.

Tekin, H.O., Kara, U., 2016. Monte Carlo simulation for distance and absorbed dose calculations in a PET-CT facility by using MCNP-X. J. Commun. Comput. 13, 32–35. http://dx.doi.org/10.17265/1548-7709/2016.01.005.

Tekin, H.O., Singh, V.P., Kara, U., Manici, T., Altunsoy, E.E., 2016. Investigation of nanoparticle effect on radiation shielding property using Monte Carlo method. CBU J. Sci. 12 (2), 196–200. http://dx.doi.org/10.18466/cbujos.92713.

Wasmi, B.A., Al-Amiery, A.A., Kadhum, A.A.H., Mohamad, A.B., 2014. Novel approach: tungsten oxide nanoparticle as a catalyst for malonic acid ester synthesis via ozonolysis. J. Nanomater. http://dx.doi.org/10.1155/2014/715457.